ELSEVIER

International Journal of Solids and Structures 41 (2004) 3193–3209

INTERNATIONAL JOURNAL OF SOLIDS and STRUCTURES

www.elsevier.com/locate/ijsolstr

# Dynamic behavior of a piezoelectric ceramic layer with two surface cracks

Xian-Fang Li [a,b,*], Kang Yong Lee [c]

[a] *Institute of Mechanics and Sensor Technology, School of Civil Engineering and Architecture, Central South University, Changsha, Hunan 410083, PR China*

[b] *College of Mathematics and Computer Science, Hunan Normal University, Changsha 410081, PR China*

[c] *School of Mechanical Engineering, Yonsei University, Seoul 120-749, South Korea*

Received 14 May 2003; received in revised form 13 December 2003

Available online 7 February 2004

**Abstract**

The transient response of a transversely isotropic piezoelectric ceramic layer containing two surface cracks is analyzed under the action of antiplane mechanical and inplane electric impacts. By using the Laplace transform and the finite Fourier transform, the mixed initial-boundary-value problem is reduced to singular integral equations of the first kind. The Lobatto–Chebyshev collocation technique is employed to solve numerically the resulting singular integral equations, and dynamic field intensity factors and strain energy release rate are determined for both permeable and impermeable cracks. Performing the inverse Laplace transform, numerical results are presented graphically to show the effects of the geometric parameters, and the material properties on the dynamic strain energy release rate. The dynamic interaction of two surface cracks, and cracks with free surfaces is discussed in detail.



*Keywords:* Surface crack; Transient analysis; Piezoelectric layer; Strain energy release rate

## 1. Introduction

As a class of smart materials, piezoelectric ceramics have been widely used in adaptive microelectromechanical systems such as sensors, actuators, and transducers due to a strong coupling characteristic between elastic and electric behaviors (Rao and Sunar, 1994; Uchino, 1998). Now, piezoelectric sensors, actuators, and transducers of various configurations can be manufactured for specified functions (Tsou and Bergman, 1998). For example, in signal processing applications, with the aid of excitation or reception of

* Corresponding author. Address: College of Mathematics and Computer Science, Hunan Normal University, Changsha, Hunan 410081, PR China.

*E-mail addresses:* xfli00@china.com.cn (X.-F. Li), kyl2813@yahoo.co.kr (K.Y. Lee).

0020-7683/$ - see front matter © 2004 Elsevier Ltd. All rights reserved.
doi:10.1016/j.ijsolstr.2003.12.016

the surface acoustic waves, an interdigital transducer is a thin piezoelectric layer bonded perfectly on a elastic substrate. And on the surface of the piezoelectric film, an array of electrodes is arranged according to different patterns (Dieulesaint and Royer, 1980).

On the other hand, a disadvantage of piezoelectric ceramics is that they are very brittle and has low strength, so they are susceptive to fracture. In recent years, the study of the reliability of piezoelectric ceramics with defects has become an intensive subject of investigation (Suo et al., 1992; Yang, 2001). In particular, since piezoelectric structures usually operate in environment relating to time-dependent loadings, the dynamic response problem of mechanical and electrical behaviors in a cracked piezoelectric ceramic under various time-dependent loadings is of great significance. Along this line, many efforts in this field have been made in theory to analyze the responses of the electric and elastic fields disturbed by cracks in a piezoelectric material subjected to dynamic electromechanical loadings. The dynamic Green's functions for anisotropic piezoelectric materials have been formulated by Narris (1994). The fundamental solutions for dynamic piezoelectricity equations of piezoelectric materials have been derived by Khutoryansky and Sosa (1995), Sosa and Khutoryansky (2001). For a cracked piezoelectric material under the action of time-dependent electromechanical loadings, Dascalu and Maugin (1995) studied the dynamic problem of crack propagation in a self-similar manner in a piezoelectric material by the quasielectrostatic approximation method. The dynamic electroelastic behavior of a piezoelectric material has been analyzed for a semi-infinite moving crack subjected to impact loads by Li and Mataga (1996a,b) with the electrode boundary condition and the vacuum boundary condition at the crack faces, respectively. For a semi-infinite stationary crack in a piezoelectric material subjected to a concentrated electromechanical impact at the crack faces, a closed-form solution has been derived for an impermeable crack by Li (2001). Generally speaking, a crack in a piezoelectric material is commonly of finite length. In this case, electroelastic field under electromechanical impacts acting on the crack faces, in particular the effect of electric impact on elastic behavior, has been analyzed by Shindo et al. (1999) for mode-I crack, who determined numerically the dynamic stress intensity factor and the dynamic energy release rate under the electrically permeable assumption, and by Chen and Karihaloo (1999) for mode-III crack, who gave some numerical results on the dynamic stress intensity factor for an impermeable crack. Some similar dynamic problems in a piezoelectric strip containing transverse or longitudinal internal crack(s) have further been investigated under the electrically permeable or impermeable assumption (Chen and Meguid, 2000; Wang and Yu, 2000; Meguid and Chen, 2001; Shin et al., 2001; Gu et al., 2002; Li and Fan, 2002; Li and Tang, 2003).

For multiple mode-III cracks in a non-homogeneous smart laminate material, the dynamic analysis has been proposed via integral transform approaches by Wang et al. (1998), Wang and Noda (2001). Recently, Meguid and Zhao (2002) considered antiplane shear crack situated at the interface a piezoelectric strip bonded to an elastic half-space subjected to dynamic impacts, and studied electroelastic response under permeable and impermeable assumptions. They found that electric-displacement intensity factors for an impermeable crack exhibit a transient feature, and depend on time, which is contrast to the existing results. However, it should be pointed out that this conclusion is based on the adopted boundary conditions at the surfaces of the crack, which are different from the previous.

This paper is concerned with the transient problem of a piezoelectric layer with two surface cracks subjected to sudden electromechanical impact. The dynamic interaction of two surface cracks is analyzed for the case of antiplane mechanical and inplane electric excitations. The Laplace transform and the finite Fourier transform are employed to reduce the mixed initial-boundary-value problem to singular integral equations with Cauchy kernel of the first kind. Based on the Lobatto–Chebyshev collocation quadrature technique, the resulting singular integral equations are solved numerically. The dynamic strain energy release rate (SERR) is obtained both for permeable and impermeable cracks by a numerical inversion of the Laplace transform. The effects of the geometric parameters and the material properties are examined in detail.

## 2. Statement of the problem

For a typical actuator composed of a thin piezoelectric ceramic layer, it is assumed that the piezoelectric layer is transversely isotropic. The problem to be considered is depicted in Fig. 1, where Cartesian coordinates $x, y, z$ are the principal axes of the material symmetry while the $z$-axis is oriented in the poling direction of the piezoelectric ceramic, which is not depicted in Fig. 1. The thickness of the piezoelectric ceramic layer is assumed to be $h$, and two surface cracks of equal length and spaced by distance $d$ occupy the regions $0 \leqslant x \leqslant a,\ y = \pm d/2,\ -\infty < z < \infty$. For a piezoelectric actuator, an external electric field is usually applied to parallel to the poling direction of the piezoelectric material, which gives rise to elastic displacements parallel to and perpendicular to the poling axis. In other words, under such circumstances, piezoelectric ceramics undergo expansion or shrinkage. However, a recent experiment by Mueller and Zhang (1998) showed that shear strain response of piezoelectric ceramics under the action of an external electric field perpendicular to the poling axis can be exploited to design new piezoelectric actuators. In the following analysis, special attention is paid to the latter case.

From the viewpoint of fracture mechanics, of much significancy is the singular field near a crack tip. Hence, in the present study we consider the case where sudden impacts are simultaneously exerted at the crack faces. Within the framework of the theory of linear piezoelectricity, the constitutive equations in the piezoelectric ceramic take the forms

$$\sigma_{ij} = c_{ijkl}s_{kl} - e_{kij}E_k, \qquad D_i = e_{ikl}s_{kl} + \varepsilon_{ik}E_k. \tag{1}$$

When subjected to sudden antiplane mechanical and inplane electric impacts, the piezoelectric ceramic layer is in a state of longitudinal shear deformation. In this case, the antiplane deformation is coupled with the inplane electric field, and the corresponding constitutive equations reduce to

$$\tau_{zx} = c_{44}^{\mathrm{E}}\gamma_{zx} - e_{15}E_x, \qquad \tau_{zy} = c_{44}^{\mathrm{E}}\gamma_{zy} - e_{15}E_y, \tag{2}$$

$$D_x = e_{15}\gamma_{zx} + \varepsilon_{11}E_x, \qquad D_y = e_{15}\gamma_{zy} + \varepsilon_{11}E_y, \tag{3}$$

where $c_{44}^{\mathrm{E}}$, $\varepsilon_{11}$, and $e_{15}$ are the elastic stiffness measured in a constant electric field, the dielectric permittivity measured at a uniform strain, the piezoelectric constant, respectively, $\tau$, $\gamma$, $D$, and $E$ are stress, strain, electric displacement, and electric field, respectively. Here strain and electric field can be determined in terms of the out-of-plane displacement $w(x, y, t)$ and inplane electric potential $\phi(x, y, t)$, by the following gradient relations

$$\gamma_{zx} = w_{,x}, \qquad \gamma_{zy} = w_{,y}, \tag{4}$$

$$E_x = -\phi_{,x}, \qquad E_y = -\phi_{,y}, \tag{5}$$

where the comma following a function denotes partial differentiation with respect to the suffix space variable.

From the equation of motion and the equilibrium equation of charges, neglecting body forces and free charges, it follows that $w(x, y, t)$ and $\phi(x, y, t)$ satisfy the basic governing partial differential equations

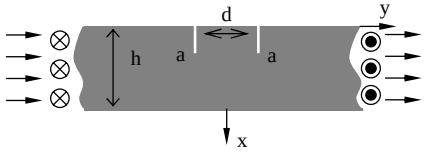


Fig. 1. Schematic of a piezoelectric ceramic layer with two surface cracks.

$$c_{44}^{\mathrm{E}}\nabla^2 w + e_{15}\nabla^2\phi = \rho\frac{\partial^2 w}{\partial t^2}, \qquad e_{15}\nabla^2 w - \varepsilon_{11}\nabla^2\phi = 0, \tag{6}$$

where $\rho$ is the mass density of the piezoelectric ceramic, and $\nabla^2$ represents the two-dimensional Laplacian operator.

The relevant mechanical and electric boundary conditions are given as follows. The layer boundary surfaces are clearly free of stress and of electric displacement, which can be stated as below

$$\tau_{zx}(0,y,t) = 0, \quad \tau_{zx}(h,y,t) = 0, \qquad -\infty < y < \infty,\ t > 0, \tag{7}$$

$$D_x(0,y,t) = 0, \quad D_x(h,y,t) = 0, \qquad -\infty < y < \infty,\ t > 0. \tag{8}$$

Apart from the above boundary conditions at the layer surfaces, appropriate boundary conditions at the crack faces must be furnished. For elastic part, obviously, we have

$$\tau_{zy}(x,\pm d/2,t) = -\tau_0 f_m(t), \quad 0 < x < a,\ t > 0, \tag{9}$$

where $f_m(t) = 0$ as $t \leqslant 0$, and $\tau_0$ is a prescribed constant. However, there are some controversial arguments for electric boundary conditions at the crack faces, one opinion assuming that the crack is permeable to electric field (Shindo et al., 1999; Kwon and Lee, 2001, etc.), and another assuming that the crack is impermeable to electric field (Pak, 1990; Chen and Karihaloo, 1999, etc.). Consequently, electric boundary conditions at the crack faces can be stated as

$$\phi^+(x,\pm d/2,t) = \phi^-(x,\pm d/2,t), \quad D_y^+(x,\pm d/2,t) = D_y^-(x,\pm d/2,t), \quad 0 \leqslant x \leqslant a,\ t > 0 \tag{10}$$

for the permeable assumption, or

$$D_y(x,\pm d/2,t) = -D_0 f_e(t), \quad 0 < x < a,\ t > 0 \tag{11}$$

for the impermeable assumption, where $f_e(t) = 0$ as $t \leqslant 0$, and $D_0$ is a prescribed constant.

## 3. Derivation of the singular integral equation

Due to the symmetry of the problem, it is sufficient to consider only the region $y \geqslant 0$. So in the following we concentrate our attention to the region $y \geqslant 0$. To solve the above problem, a simplification of equations in (6) can be achieved by introducing a new function

$$\varphi = \phi - \frac{e_{15}}{\varepsilon_{11}} w. \tag{12}$$

Hence, equations in (6) then become

$$\nabla^2 w = \frac{1}{c_s^2}\frac{\partial^2 w}{\partial t^2}, \qquad \nabla^2\varphi = 0, \tag{13}$$

where $c_s = \sqrt{c_{44}^{\mathrm{D}}/\rho}$ denotes the shear wave velocity of a piezoelectric ceramic, $c_{44}^{\mathrm{D}} = c_{44}^{\mathrm{E}} + e_{15}^2/\varepsilon_{11}$ being the elastic stiffened constant measured under a constant electric-displacement condition. Thus, the stress and the electric displacement can be expressed in terms of $w$ and $\varphi$ as follows

$$\tau_{zx} = c_{44}^{\mathrm{D}} w_{,x} + e_{15}\varphi_{,x}, \qquad \tau_{zy} = c_{44}^{\mathrm{D}} w_{,y} + e_{15}\varphi_{,y}, \tag{14}$$

$$D_x = -\varepsilon_{11}\varphi_{,x}, \qquad D_y = -\varepsilon_{11}\varphi_{,y}. \tag{15}$$

Suppose that the piezoelectric ceramic is at rest initially. Application of the Laplace transform to the equations in (13) leads to partial differential equations without $t$. Then, using the finite Fourier transform to

these equations, it is easy to verify that an appropriate solution of equations in (13) in the Laplace transform domain, satisfying (7) and (8), may be written in a Fourier series of the form

$$\tilde{w}^{\mathrm{I}}(x,y,p) = A_0^{\mathrm{I}}(p)\exp\left[\frac{p}{c_s}\left(\frac{d}{2}-y\right)\right] + \sum_{n=1}^{\infty} A_n^{\mathrm{I}}(p)\exp\left[n\beta\alpha_n\left(\frac{d}{2}-y\right)\right]\cos(n\beta x), \tag{16}$$

$$\tilde{\varphi}^{\mathrm{I}}(x,y,p) = B_0^{\mathrm{I}}(p) + \sum_{n=1}^{\infty} B_n^{\mathrm{I}}(p)\exp\left[n\beta\left(\frac{d}{2}-y\right)\right]\cos(n\beta x) \tag{17}$$

for $0 \leqslant x \leqslant h$, $y \geqslant d/2$, and

$$\tilde{w}^{\mathrm{II}}(x,y,p) = A_0^{\mathrm{II}}(p)\frac{\sinh\left(\frac{p}{c_s}y\right)}{\sinh\left(\frac{pd}{2c_s}\right)} + \sum_{n=1}^{\infty} A_n^{\mathrm{II}}(p)\frac{\sinh(n\beta\alpha_n y)}{\sinh\left(\frac{n\beta\alpha_n d}{2}\right)}\cos(n\beta x), \tag{18}$$

$$\tilde{\varphi}^{\mathrm{II}}(x,y,p) = \sum_{n=1}^{\infty} B_n^{\mathrm{II}}(p)\frac{\sinh(n\beta y)}{\sinh\left(\frac{n\beta d}{2}\right)}\cos(n\beta x) \tag{19}$$

for $0 \leqslant x \leqslant h$, $0 \leqslant y \leqslant d/2$, with

$$\alpha_n = \sqrt{1+\left(\frac{hp}{n\pi c_s}\right)^2}, \quad \beta = \frac{\pi}{h}, \tag{20}$$

where a variable with the superscripts I or II specifies the variable in the region $y \geqslant d/2$ and in the region $0 \leqslant y \leqslant d/2$, respectively, and $A_n^{\mathrm{J}}(p)$ and $B_n^{\mathrm{J}}(p)$ $(n = 0, 1, 2, \ldots)$ $(\mathrm{J} = \mathrm{I}, \mathrm{II})$ are unknown functions to be determined. Here the wave over a function denotes the Laplace transform of this function with respect to $t$, and $p$ is the Laplace transform parameter.

Furthermore, from (14) and (15) it is not difficult to obtain expressions for the components of stress and electric displacement in the Laplace transform domain, which are omitted for saving space. In particular, for $y = d/2$ we get

$$\tilde{\tau}_{zy}^{\mathrm{I}}(x,d/2,p) = -\frac{c_{44}^{\mathrm{D}}p}{c_s}A_0^{\mathrm{I}} - \beta\sum_{n=1}^{\infty} n[c_{44}^{\mathrm{D}}\alpha_n A_n^{\mathrm{I}} + e_{15}B_n^{\mathrm{I}}]\cos(n\beta x), \tag{21}$$

$$\tilde{\tau}_{zy}^{\mathrm{II}}(x,d/2,p) = \frac{c_{44}^{\mathrm{D}}p}{c_s}A_0^{\mathrm{II}}\coth\left(\frac{pd}{2c_s}\right) + \beta\sum_{n=1}^{\infty} n\left[c_{44}^{\mathrm{D}}\alpha_n A_n^{\mathrm{II}}\coth\left(\frac{n\beta d\alpha_n}{2}\right) + e_{15}B_n^{\mathrm{II}}\coth\left(\frac{n\beta d}{2}\right)\right]\cos(n\beta x), \tag{22}$$

$$\widetilde{D}_y^{\mathrm{I}}(x,d/2,p) = \varepsilon_{11}\beta\sum_{n=1}^{\infty} nB_n^{\mathrm{I}}\cos(n\beta x), \tag{23}$$

$$\widetilde{D}_y^{\mathrm{II}}(x,d/2,p) = -\varepsilon_{11}\beta\sum_{n=1}^{\infty} nB_n^{\mathrm{II}}\coth\left(\frac{n\beta d}{2}\right)\cos(n\beta x) \tag{24}$$

for $0 \leqslant x \leqslant h$.

Our aim is to determine the transient behavior in a cracked piezoelectric layer, in particular in the vicinity of the crack tip. Consequently, in the following, we do not seek directly $A_n^{\mathrm{I}}$, $A_n^{\mathrm{II}}$, $B_n^{\mathrm{I}}$, and $B_n^{\mathrm{II}}$. Instead, we introduce two new unknown functions as follows

$$g(x,t)=\frac{1}{2}\frac{\partial[\Delta w(x,t)]}{\partial x},\qquad h(x,t)=\frac{1}{2}\frac{\partial[\Delta\varphi(x,t)]}{\partial x}, \tag{25}$$

where

$$\Delta w(x,t)=w^{\mathrm{I}}(x,d/2,t)-w^{\mathrm{II}}(x,d/2,t), \tag{26}$$

$$\Delta\varphi(x,t)=\varphi^{\mathrm{I}}(x,d/2,t)-\varphi^{\mathrm{II}}(x,d/2,t). \tag{27}$$

Eliminating these unknown $A_n^{\mathrm{I}}$, $A_n^{\mathrm{II}}$, $B_n^{\mathrm{I}}$, and $B_n^{\mathrm{II}}$ from given boundary conditions leads to singular integral equations. To this end, at first, the continuity of the stress and the electric displacement at $y=d/2$ allows us to get

$$A_0^{\mathrm{II}}=-A_0^{\mathrm{I}}\tanh\left(\frac{pd}{2c_s}\right), \tag{28}$$

$$A_n^{\mathrm{II}}=-A_n^{\mathrm{I}}\tanh\left(\frac{n\beta d\alpha_n}{2}\right),\quad B_n^{\mathrm{II}}=-B_n^{\mathrm{I}}\tanh\left(\frac{n\beta d}{2}\right),\qquad n=1,2,\ldots \tag{29}$$

These results are inserted into (16)–(19), and a simple evaluation yields

$$\Delta\tilde{w}(x,p)=A_0^{\mathrm{I}}\left[1+\tanh\left(\frac{pd}{2c_s}\right)\right]+\sum_{n=1}^{\infty}A_n^{\mathrm{I}}\left[1+\tanh\left(\frac{n\beta d\alpha_n}{2}\right)\right]\cos(n\beta x), \tag{30}$$

$$\Delta\tilde{\varphi}(x,p)=B_0^{\mathrm{I}}+\sum_{n=1}^{\infty}B_n^{\mathrm{I}}\left[1+\tanh\left(\frac{n\beta d}{2}\right)\right]\cos(n\beta x) \tag{31}$$

for $0\leqslant x\leqslant h$. In the following, we consider a permeable and impermeable case, respectively.

### 3.1. Permeable case

With the help of the electric boundary condition (10), in connection with the continuity of electric potential at the bonding of the regions I and II, i.e. $a\leqslant x\leqslant h$, $y=d/2$, taking into account (12), we derive

$$B_0^{\mathrm{I}}=-\frac{e_{15}}{\varepsilon_{11}}A_0^{\mathrm{I}}\left[1+\tanh\left(\frac{pd}{2c_s}\right)\right], \tag{32}$$

$$B_n^{\mathrm{I}}\left[1+\tanh\left(\frac{n\beta d}{2}\right)\right]=-\frac{e_{15}}{\varepsilon_{11}}A_n^{\mathrm{I}}\left[1+\tanh\left(\frac{n\beta d\alpha_n}{2}\right)\right],\qquad n=1,2,\ldots \tag{33}$$

On the other hand, by using (21), application of the Laplace transform to the elastic boundary condition (9) yields

$$\frac{c_{44}^{\mathrm{D}}p}{c_s}A_0^{\mathrm{I}}+\beta\sum_{n=1}^{\infty}n[c_{44}^{\mathrm{D}}\alpha_nA_n^{\mathrm{I}}+e_{15}B_n^{\mathrm{I}}]\cos(n\beta x)=\tau_0\tilde{f}_m(p),\quad 0<x<a. \tag{34}$$

Furthermore, use of the condition $\Delta w(x,t)=0$, $a\leqslant x\leqslant h$, allows us to eliminate $A_n^{\mathrm{I}}$ and $B_n^{\mathrm{I}}$. For this purpose, if we choose $A_n^{\mathrm{I}}$ represented in terms of the following integrals

$$A_0^{\mathrm{I}}\left[1+\tanh\left(\frac{pd}{2c_s}\right)\right]=-\frac{2}{h}\int_0^a s\tilde{g}(s,p)\,\mathrm{d}s, \tag{35}$$

$$A_n^{\mathrm{I}}\left[1+\tanh\left(\frac{n\beta d\alpha_n}{2}\right)\right]=-\frac{4}{nh\beta}\int_0^a\tilde{g}(s,p)\sin(n\beta s)\,\mathrm{d}s,\quad n=1,2,\ldots, \tag{36}$$

recalling the known result

$$\frac{s}{2}+\sum_{n=1}^{\infty}\frac{1}{n}\sin(ns)\cos(nx)=\begin{cases}\frac{\pi}{2}, & 0<x<s,\\ \frac{\pi}{4}, & x=s,\\ 0, & s<x<\pi,\end{cases} \tag{37}$$

we find that $\Delta w(x,t)=0$ is automatically satisfied for $a\leqslant x\leqslant h$. On the other hand, substituting (35) and (36) into (34) yields a singular integral equation for $\tilde{g}(s,p)$

$$\frac{1}{h}\int_0^a \frac{\tilde{g}(s,p)\sin(\beta s)}{\cos(\beta s)-\cos(\beta x)}\,\mathrm{d}s-\frac{1}{h}\int_0^a \tilde{g}(s,p)T_{\mathrm{P}}(s,x,p)\,\mathrm{d}s=\frac{\tau_0}{c_{44}^{\mathrm{E}}}\tilde{f}_m(p),\quad 0<x<a \tag{38}$$

with

$$T_{\mathrm{P}}(s,x,p)=\frac{1}{1-k_e^2}\left\{\frac{ps}{c_s}\frac{2}{1+\tanh\left(\frac{pd}{2c_s}\right)}+2\sum_{n=1}^{\infty}\left[\frac{2\alpha_n}{1+\tanh(n\beta\alpha_n d/2)}-1-k_e^2\frac{1-\tanh(n\beta d/2)}{1+\tanh(n\beta d/2)}\right]\sin(n\beta s)\cos(n\beta x)\right\}, \tag{39}$$

where $k_e=e_{15}/\sqrt{c_{44}^{\mathrm{D}}\varepsilon_{11}}$ is the electromechanical coupling coefficient, which may be defined by $k_e'=e_{15}/\sqrt{c_{44}^{\mathrm{E}}\varepsilon_{11}}$ in other literature. In the above derivation, the known result

$$\sum_{n=1}^{\infty}\sin(ns)\cos(nx)=\frac{1}{2}\frac{\sin(s)}{\cos(x)-\cos(s)},\quad 0<s,\ x<\pi \tag{40}$$

has been utilized.

In particular, if the distance between two cracks is large enough, that is, setting $d\to\infty$, the governing singular integral equation does not change except for the kernel $T_{\mathrm{P}}$ replaced by

$$T_{\mathrm{P}}(s,x,p)=\frac{1}{1-k_e^2}\left[\frac{ps}{c_s}+2\sum_{n=1}^{\infty}(\alpha_n-1)\sin(n\beta s)\cos(n\beta x)\right]. \tag{41}$$

Additionally, if imposing $p\to 0$, the kernel $T_{\mathrm{P}}(s,x,p)$ appearing in (38) simplifies to

$$T_{\mathrm{P}}(s,x,p)=2\sum_{n=1}^{\infty}\frac{1-\tanh(n\beta d/2)}{1+\tanh(n\beta d/2)}\sin(n\beta s)\cos(n\beta x), \tag{42}$$

independent of all the material constants, and in this case the solution of (38) corresponds to the one in the static case ($t\to\infty$). Furthermore, the kernel $T_{\mathrm{P}}(s,x,p)$ in (42) vanishes if $d\to\infty$. For the latter, the equation is solvable analytically, and the solution may be determined in a closed form.

### 3.2. Impermeable case

For this case, making use of the impermeable electric boundary condition (11) instead of (10) and omitting the detailed procedure, in a similar manner one can derive the following equations for unknown $\tilde{g}(s,p)$ and $\tilde{h}(s,p)$, respectively,

$$\frac{1}{h}\int_0^a \frac{\tilde{g}(s,p)\sin(\beta s)}{\cos(\beta s)-\cos(\beta x)}\,\mathrm{d}s-\frac{1}{h}\int_0^a \tilde{g}(s,p)T_{\mathrm{I}}(s,x,p)\,\mathrm{d}s=\frac{1}{c_{44}^{\mathrm{D}}}\left[\tau_0\tilde{f}_m(p)+\frac{e_{15}}{\varepsilon_{11}}D_0\tilde{f}_e(p)\right], \tag{43}$$

$$\frac{1}{h}\int_0^a \frac{\tilde{h}(s,p)\sin(\beta s)}{\cos(\beta s)-\cos(\beta x)}\,\mathrm{d}s - \frac{1}{h}\int_0^a \tilde{h}(s,p)T_{\mathrm{D}}(s,x,p)\,\mathrm{d}s = -\frac{1}{\varepsilon_{11}}D_0\tilde{f}_e(p) \tag{44}$$

for $0 < x < a$, with

$$T_{\mathrm{I}}(s,x,p) = \frac{ps}{c_s}\frac{2}{1+\tanh\left(\frac{pd}{2c_s}\right)} + 2\sum_{n=1}^{\infty}\left[\frac{2\alpha_n}{1+\tanh(n\beta\alpha_n d/2)} - 1\right]\sin(n\beta s)\cos(n\beta x), \tag{45}$$

$$T_{\mathrm{D}}(s,x,p) = 2\sum_{n=1}^{\infty}\frac{1-\tanh(n\beta d/2)}{1+\tanh(n\beta d/2)}\sin(n\beta s)\cos(n\beta x). \tag{46}$$

For the case of a surface crack in a piezoelectric ceramic layer, it is sufficient to set $d \to \infty$. That is, the interaction of two cracks is negligible when the distance between two cracks is very large. In this case, the above kernels reduce to

$$T_{\mathrm{I}}(s,x,p) = \frac{ps}{c_s} + 2\sum_{n=1}^{\infty}(\alpha_n - 1)\sin(n\beta s)\cos(n\beta x), \tag{47}$$

$$T_{\mathrm{D}}(s,x,p) = 0. \tag{48}$$

Further, the solution of the corresponding static case ($t \to \infty$) can be easily obtained via solving analytically the equations corresponding to $p \to 0$ since in this case the kernel $T_{\mathrm{I}}(s,x,p) = 0$.

## 4. Solution of the problem

Generally speaking, the dynamic solution cannot be obtained analytically due to the complexity of the form of the kernels appearing the resulting singular integral equations. Therefore, in what follows we appeal to numerical schemes to solve these singular integral equations. To this end, introducing the dimensionless notations

$$\bar{s} = 2\frac{s}{a} - 1, \qquad \bar{x} = 2\frac{x}{a} - 1, \tag{49}$$

which are substituted into Eq. (38), then we find

$$\frac{a}{2h}\int_{-1}^{1}\frac{\tilde{g}(\bar{s},p)\sin\left(\frac{\bar{s}+1}{2}a\beta\right)}{\cos\left(\frac{\bar{s}+1}{2}a\beta\right)-\cos\left(\frac{\bar{x}+1}{2}a\beta\right)}\mathrm{d}\bar{s} - \frac{a}{2h}\int_{-1}^{1}\tilde{g}(\bar{s},p)T_{\mathrm{P}}\left(\frac{\bar{s}+1}{2}a,,\frac{\bar{x}+1}{2}a,p\right)\mathrm{d}\bar{s} = \frac{\tau_0}{c_{44}^{\mathrm{E}}}\tilde{f}_m(p) \tag{50}$$

for $-1 < \bar{x} < 1$, where we still denote the unknown as $\tilde{g}(\bar{s},p)$ for convenience, but understood as

$$\tilde{g}(\bar{s},p) = \tilde{g}\left(\frac{\bar{s}+1}{2}a,p\right). \tag{51}$$

A further simplification can be achieved by using the following results

$$\frac{a\beta\sin\left(\frac{\bar{s}+1}{2}a\beta\right)}{2\left[\cos\left(\frac{\bar{s}+1}{2}a\beta\right)-\cos\left(\frac{\bar{x}+1}{2}a\beta\right)\right]} + \frac{1}{\bar{s}-\bar{x}} \to 0 \quad \text{as } \bar{s} \to \bar{x}, \tag{52}$$

$$\beta = \frac{\pi}{h}, \tag{53}$$

and the above equation can be then rewritten as a normalized form over the interval $(-1,1)$:

$$\frac{1}{\pi}\int_{-1}^{1}\frac{\tilde{g}(\bar{s},p)}{\bar{s}-\bar{x}}\,\mathrm{d}\bar{s}+\frac{1}{\pi}\int_{-1}^{1}\tilde{g}(\bar{s},p)R_{\mathrm{P}}(\bar{s},\bar{x},p)\,\mathrm{d}\bar{s}=-\frac{\tau_0}{c_{44}^{\mathrm{E}}}\tilde{f}_m(p),\quad -1<\bar{x}<1, \tag{54}$$

where the kernel

$$R_{\mathrm{P}}(\bar{s},\bar{x},p)=\frac{a\beta}{2}T_{\mathrm{P}}\left(\frac{\bar{s}+1}{2}a,\frac{\bar{x}+1}{2}a,p\right)-\frac{a\beta\sin\left(\frac{\bar{s}+1}{2}a\beta\right)}{2\left[\cos\left(\frac{\bar{s}+1}{2}a\beta\right)-\cos\left(\frac{\bar{x}+1}{2}a\beta\right)\right]}-\frac{1}{\bar{s}-\bar{x}} \tag{55}$$

is bounded, and does not have any singularity even for $\bar{s}\to\bar{x}$. The singular part of the kernel appears only in the first term at the left-hand side of Eq. (54), so Eq. (54) is a standard singular integral equation with Cauchy kernel. The numerical solution can be attacked by the technique established by Erdogan et al. (1973) and further developed by Theocaris and Ioakimids (1977). Because of the same form of the resulting singular integral equations, the treatment of other two equations (43) and (44) is completely analogous, and omitted.

Following Erdogan et al. (1973), $\tilde{g}(\bar{x},p)$ may be assumed to take the form according to the variable $\bar{x}$

$$\tilde{g}(\bar{x},p)=-\frac{\sqrt{2}\Omega(\bar{x},p)\tau_0}{c_{44}^{\mathrm{E}}\sqrt{1-\bar{x}^2}}, \tag{56}$$

where $\Omega(\bar{x},p)$ is a bounded continuous function in the interval $-1\leqslant\bar{x}\leqslant 1$, which is obtainable by existing approaches, and the negative sign and $\sqrt{2}$ at the right-hand side are introduced for convenience. Furthermore, in view of $g(x,t)=(\Delta w)_{,x}/2$, from the physical considerations, $\tilde{g}(x,p)$ in $0<x<a$ must have singularity at the crack tip $x=a$, and has no any singularity at the crack mouth $x=0$. Hence, in order to avoid the occurrence of a singularity at the crack mouth, one may impose an artificial constraint for $\tilde{g}(\bar{x},p)$,

$$\Omega(-1,p)=0. \tag{57}$$

In what follows the Lobatto–Chebyshev collocation method developed by Theocaris and Ioakimids (1977) is utilized to determinate a numerical solution of Eq. (54). It is worth noting that this method has a remarkable advantage as compared to the Gauss–Chebyshev collocation method (Erdogan et al., 1973), since field intensity factors at the crack tip are obtained directly for the former case, and evaluated with a complementary procedure such as extrapolation based on the determined internal values for the latter case. Accordingly, by employing the quadrature formula

$$\frac{1}{\pi}\int_{-1}^{1}\frac{1}{\bar{s}-\bar{x}_j}\frac{\Omega(\bar{s})}{\sqrt{1-\bar{s}^2}}\,\mathrm{d}\bar{s}\simeq\frac{1}{n}\sum_{i=0}^{n}\lambda_i\frac{\Omega(\bar{s}_i)}{\bar{s}_i-\bar{x}_j}, \tag{58}$$

where $\bar{x}_j=\cos[(2j-1)\pi/2n]$, $\bar{s}_i=\cos(i\pi/n)$, $(j=1,2,\ldots,n, i=0,1,\ldots,n)$, $\lambda_0=\lambda_n=1/2$, $\lambda_1=\cdots=\lambda_{n-1}=1$, Eq. (54) subjected to the constraint (57) is approximated by the following system of $n+1$ linear algebraic equations in $n+1$ unknown $\Omega(\bar{s}_i)$ $(i=0,1,\ldots,n)$:

$$\frac{1}{n}\sum_{i=0}^{n}\lambda_i\frac{\Omega(\bar{s}_i)}{\bar{s}_i-\bar{x}_j}+\frac{1}{n}\sum_{i=0}^{n}\lambda_i R_{\mathrm{P}}(\bar{s}_i,\bar{x}_j,p)\Omega(\bar{s}_i)=\frac{1}{\sqrt{2}}\tilde{f}_m(p),\quad j=1,2,\ldots,n, \tag{59}$$

$$\Omega(-1)=0, \tag{60}$$

where we have omitted the parameter $p$ in $\Omega(\bar{s}_i,p)$, for simplicity.

The values of $\Omega(\bar{s})$ at the collocation points $\bar{s}_i$, $\Omega(\bar{s}_i)$, are therefore determined by solving the above resulting algebraic system. In particular, of much interest is $\Omega(1)$, which is directly related to or proportional

to the field intensity factors. Once $\Omega(1)$ is obtained, the dynamic stress intensity factor in the Laplace transform domain, defined by

$$K_{\mathrm{III}}^{\tau}(t) = \lim_{x \to a^{+}} \sqrt{2\pi(x-a)}\tau_{zy}^{\mathrm{I}}(x,0,t) \tag{61}$$

can be evaluated by

$$\widetilde{K}_{\mathrm{III}}^{\tau}(p) = \Omega_{\mathrm{P}}(1)\tau_0\sqrt{\pi a}, \tag{62}$$

for permeable surface cracks, or

$$\widetilde{K}_{\mathrm{III}}^{\tau}(p) = \left\{\tau_0\Omega_{\mathrm{I}}(1) + \frac{e_{15}}{\varepsilon_{11}}D_0[\Omega_{\mathrm{I}}(1) - \Omega_{\mathrm{D}}(1)]\right\}\sqrt{\pi a} \tag{63}$$

for impermeable surface cracks. Here $\Omega(1)$ with a subscript stands for the solution to Eq. (54) corresponding to the kernel with the same subscript.

Similar treatment can arrive at the electric-displacement intensity factors. It indicates that the stress and the electric-displacement for each case exhibit a usual square-root singularity, but the corresponding intensity factors have different relationships of dependence. That is, the intensity factors of stress and electric-displacement depend only on mechanical impact, not on electric impact for permeable cracks, whereas the stress intensity factors depend not only on mechanical impact, but also on electric impact for impermeable cracks. However, the electric-displacement intensity factors are independent of mechanical impact for impermeable cracks. In effect, taking into account the fact that time $t$ does not appear in the kernel $T_{\mathrm{D}}(s,x,p)$, application of the inverse Laplace transform to Eq. (44) yields an equation in time domain, and so we have

$$K^{\mathrm{D}}(t) = -f_e(t)\Omega_{\mathrm{D}}(1)D_0\sqrt{\pi a}, \tag{64}$$

where $\Omega_{\mathrm{D}}(1)$ is the solutions relating to the equation without $t$. Note that impact loadings here refer only to those acting on the crack faces. Owing to the coupling feature between elastic and electric fields in a piezoelectric material, a mechanical impact acting on the crack faces may be produced by a remote electric excitation, and similarly an electric impact on the crack faces may be caused by a remote mechanical excitation.

In analyzing the stability of a crack in a piezoelectric material, there exist some fracture criteria in theory. Energy release rate according to the classical definition may give rise to negative values for certain combined electromechanical loadings, which lacks clear physical interpretation, while strain energy release rate (SERR) presented by Park and Sun (1995) seems to be a suitable fracture criterion for a cracked piezoelectric material since theoretical prediction based on this criterion agrees basically with the experimental data given in Park and Sun (1995). In the present study, the dynamic SERR

$$G^{S}(t) = \lim_{\delta \to 0}\frac{1}{2\delta}\int_0^{\delta}\tau_{zy}^{\mathrm{I}}(r,d/2,t)\Delta w(\delta - r,t)\,\mathrm{d}r \tag{65}$$

$r$ being the distance from the crack tip, is adopted. From the above-obtained results, for the case of $f_m(t) = f_e(t)$, a direct evaluation can derive dynamic SERR in the present study as

$$G^{S}(t) = \frac{(\tau_0)^2\pi a}{2}k^{\tau}(t)k^{\gamma}(t) \tag{66}$$

for permeable and impermeable cracks, where $k^{\tau}(t)$ and $k^{\gamma}(t)$ represent the inverse Laplace transforms of $\tilde{k}^{\tau}(p)$ and $\tilde{k}^{\gamma}(p)$, given by

$$\tilde{k}^{\tau}(p) = \begin{cases} \Omega_{\mathrm{P}}(1) & \text{for the permeable case,} \\ \Omega_{\mathrm{I}}(1) + D_m(\Omega_{\mathrm{I}}(1) - \Omega_{\mathrm{D}}(1)) & \text{for the impermeable case,} \end{cases} \tag{67}$$

and

$$\tilde{k}^{\gamma}(p) = \begin{cases} \frac{1}{c_{44}^{\mathrm{E}}}\Omega_{\mathrm{P}}(1) & \text{for the permeable case,} \\ \frac{1+D_m}{c_{44}^{\mathrm{D}}}\Omega_{\mathrm{I}}(1) & \text{for the impermeable case,} \end{cases} \tag{68}$$

where $D_m = e_{15}D_0/\varepsilon_{11}\tau_0$.

## 5. Results and discussions

In this section, numerical results for dynamic SERRs will be presented based on the above-obtained results. For this purpose, a numerical inversion of the Laplace transform (Crump, 1976) is adopted to determine $k^{\tau}(t)$ and $k^{\gamma}(t)$, and then dynamic SERRs. Numerical computations are carried out for a PZT-5H layer with two surface cracks. The relevant material constants are $c_{44}^{\mathrm{E}} = 3.53 \times 10^{10}$ N/m$^2$, $e_{15} = 17.0$ C/m$^2$, $\varepsilon_{11} = 151 \times 10^{-10}$ C/Vm, $G_{\mathrm{cr}} = 5.0$ N/m (Pak, 1990). For simplicity, impact functions $f_m(t)$ and $f_e(t)$ are chosen to be the Heaviside unit step function $H(t)$, which is frequently used in the study of fracture mechanics.

First, the effects of the material properties on the dynamic stress intensity factors are examined. From (63), along with Eqs. (43) and (44), it can be concluded that the normalized stress intensity factor $k^{\tau}(t)$ as a function of the normalized time $c_s t/a$ is independent of the material properties for impermeable cracks if treating $e_{15}D_0/\varepsilon_{11}\tau_0$ as a single independent parameter $D_m = e_{15}D_0/\varepsilon_{11}\tau_0$. However, this is not true for permeable cracks. For latter, $k_e = e_{15}/c_{44}^{\mathrm{D}}\varepsilon_{11}$ has a strong influence on the dynamic stress intensity factors. Figs. 2 and 3 display variation of the normalized dynamic stress intensity factor $k^{\tau}(t)$ against the normalized time $c_s t/a$ with $h/a = 2, 5$, respectively, for permeable surface cracks. For comparison, the corresponding results for a purely elastic medium, which may be treated as the results neglecting the piezoelectric constant $e_{15}$, are plotted in these figures. As seen from Figs. 2 and 3, a dynamic overshoot is very apparent. For a

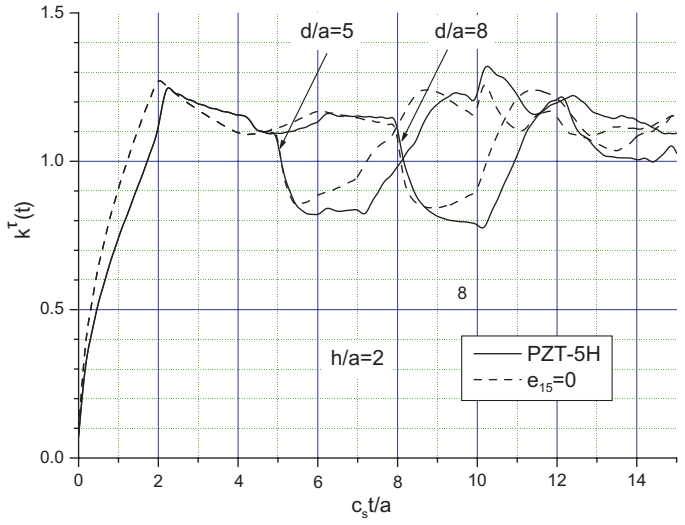


Fig. 2. $k^{\tau}(t)$ vs $c_s t/a$ with $d/a = 5$, 8 and $h/a = 2$ for a cracked PZT-5H layer.

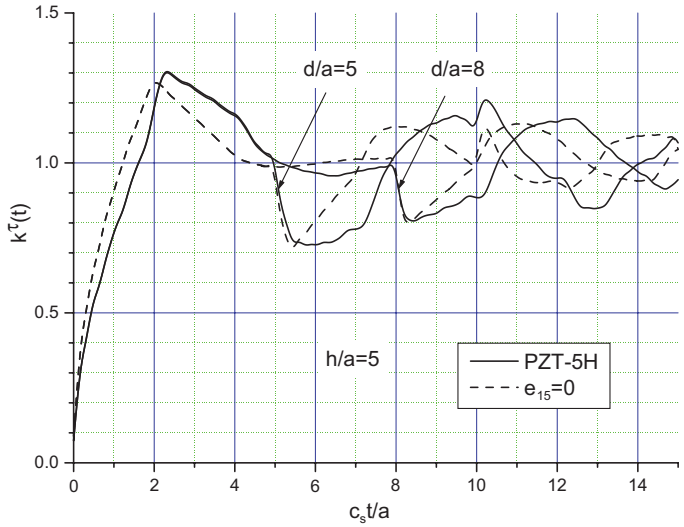


Fig. 3. $k^{\tau}(t)$ vs $c_s t/a$ with $d/a = 5$, 8 and $h/a = 5$ for a cracked PZT-5H layer.

purely elastic medium, as expected, a dynamic overshoot occurs exactly at $c_s t/a = 2$, since the waves generated at the crack faces near the crack tip are reflected through the surface $x = 0$, and arrive at again the crack tip, taking the normalized time $c_s t/a = 2$. Owing to the influence of $k_e$, a dynamic overshoot occurs later slightly than a purely elastic medium, and the magnitude is intensified or weakened depending upon $h/a$. Also expected is that the response curve of $k^{\tau}(t)$ for $d/a = 5$ is the same as that for $d/a = 8$ before the arrival of the wave-fronts generated at the crack in $y < 0$. After the arrival of these wave-fronts, the dynamic interaction of two cracks takes place. For example, it takes time $c_s t/a = 5$ for the wave-fronts, which weaken the stress intensity factors, to travel the crack tip in $y > 0$ for $d/a = 5$; so $k^{\tau}(t)$ drops immediately at $c_s t/a = 5$. As time is large enough, the effect of $k_e$ is seen to be very slight and negligible, in accordance with the fact that the static stress intensity factors are independent of material properties including $k_e$. Therefore, $k_e$ causes the delay of response of $k^{\tau}(t)$, and the peaks are intensified or weakened depending on $h/a$.

Figs. 4–6 show the dynamic SERR normalized by $(\tau_0)^2 \pi a/2G_{cr}$, denoted as $G^0(t)$, against $c_s t/a$ with $h/a = 2, 5, 8$, for three different distances between two cracks $d/a = 2, 5, 8$, respectively, for permeable cracks. In the following calculations, $\tau_0$ and $a$ are taken as $4.2 \times 10^6$ N/m$^2$ and 0.01 m. By comparison, it is found that the curves of $G^0(t)$ in Fig. 4 decreases more rapidly in a small range after $c_s t/a = 2$ than those in Figs. 5 and 6. This is due to the dynamic interaction of two cracks. The reason is that for $d/a = 2$, it takes about $c_s t/a = 2$ for the waves generated at the crack in $y < 0$, which weaken the magnitude of $G^0(t)$, to travel the crack tip in $y > 0$, while for $d/a = 5$ or 8, the waves generated at the crack in $y < 0$ do not reach the crack tip in $y > 0$ when $c_s t/a = 2$; so the curves of $G^0(t)$ in Figs. 5 and 6 look like the same before $c_s t/a < 5$. The dynamic interaction of two cracks with the free boundaries is also observed in Figs. 4–6. From these figures, it is seen that the curves of $G^0(t)$ for $h/a = 5$ are almost the same as those for $h/a = 8$ before $c_s t/a = 8$, and they deviate clearly away after $c_s t/a = 10$. This is because that for $h/a = 5$, the wave-fronts reflected through the layer surface $x = h$ reach again the crack tip, taking time $c_s t/a = 8$, and the second reflected waves through the layer surface $x = 0$ reach the crack tip, taking time $c_s t/a = 10$. Furthermore, from Fig. 6 we find that the response curves of $G^0(t)$ starting from the origin, rise rapidly, arriving at the first peak at about $c_s t/a = 2.3$, and then oscillate due to the superposition of the reflected

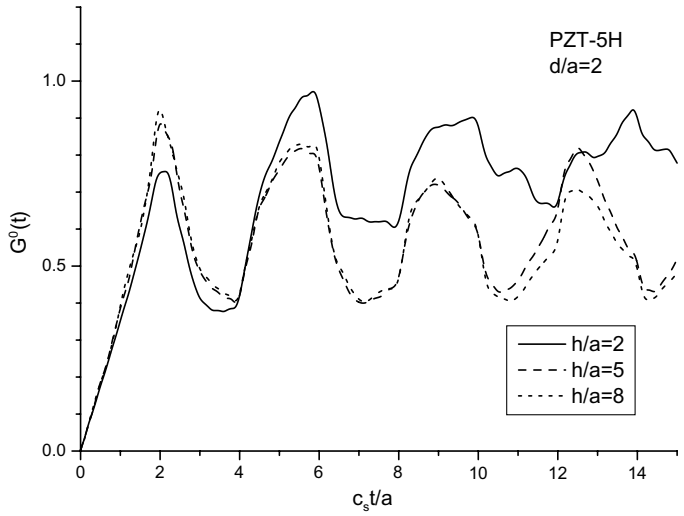


Fig. 4. Variation of $G^0(t)$ against $c_st/a$ with $d/a = 2$ and $h/a = 2, 5, 8$ under the permeable assumption.

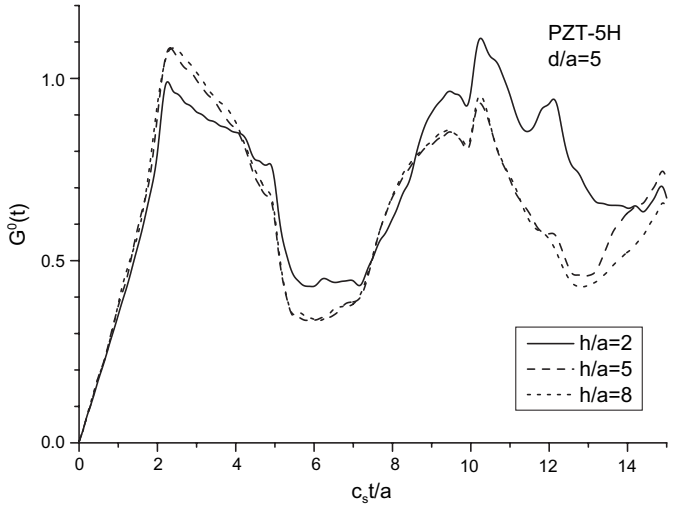


Fig. 5. Variation of $G^0(t)$ against $c_st/a$ with $d/a = 5$ and $h/a = 2, 5, 8$ under the permeable assumption.

waves through the layer surfaces and the scattering waves by two cracks, similar to Figs. 2 and 3. For example, for $d/a = 8$, the curves of $G^0(t)$ in Fig. 6 deviate slightly in a small region after $c_st/a = 4$ owing to the influence of $k_e$, and fall down immediately at $c_st/a = 8$ with the arrival of the generated waves at the other crack. After a small period of time, the scattering waves are generated and intensify the magnitude of $G^0(t)$; so $G^0(t)$ is seen to climb the second peak.

From the above, in addition to the geometric parameters, $k_e$ has a strong influence on $G^0(t)$ for permeable cracks, while electric impacts at the crack faces has no any influence of $G^0(t)$. However, for impermeable cracks, electric impacts have a pronounced contribution in $G^0(t)$. For different electric impacts, variation of $G^0(t)$ against $c_st/a$ is plotted with $h/a = 5$ and $d/a = 2, 5, 8$, in Figs. 7–9. As compared to

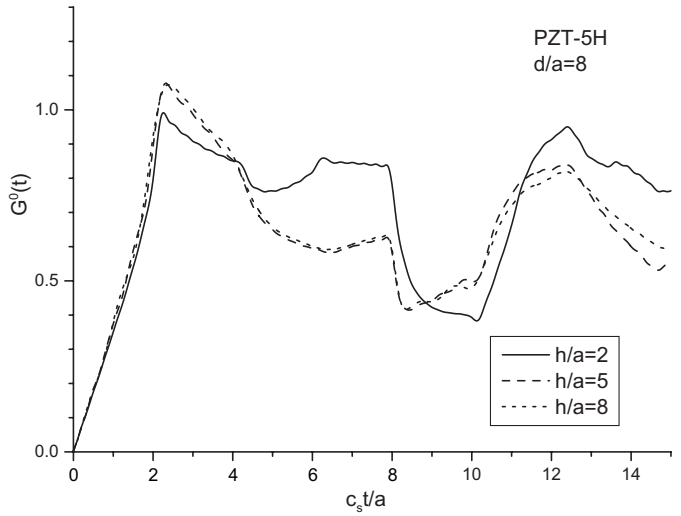


Fig. 6. Variation of $G^0(t)$ against $c_s t/a$ with $d/a = 8$ and $h/a = 2$, 5, 8 under the permeable assumption.

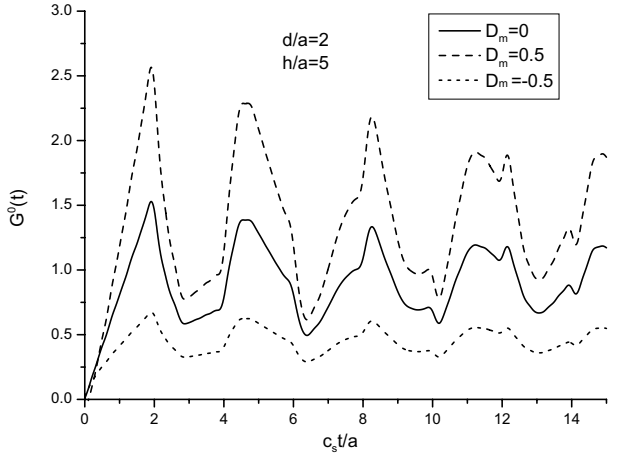


Fig. 7. Variation of $G^0(t)$ against $c_s t/a$ with $d/a = 2$, $h/a = 5$, $D_m = 0.5$, 0, −0.5 under the impermeable assumption.

permeable cracks, similar trends are observed in these figures. In particular, the curves of $G^0(t)$ rise in a straight line at the early stage of action of impacts, which agrees with the result for a piezoelectric material with a semi-infinite crack (Li, 2001), since in this stage, the reflected waves through $x = h$ and generated waves at the other crack do not arrive at the crack tip, and all the contributions in $G^0(t)$ near the crack tip arises from the waves generated at the crack itself and reflected through $x = 0$. In contrast to $G^0(t)$ for permeable cracks, for impermeable cracks $G^0(t)$ has a dynamic overshoot at exact time $c_s t/a = 2$ when $h/a > 2$ and $d/a > 2$. Moreover, the peak values decrease gradually with an increase of the number of reflected waves and scattering waves, and $G^0(t)$ approaches the corresponding static value as time tends to infinity. On the other hand, $G^0(t)$ becomes greater or lesser depending upon positive or negative electric

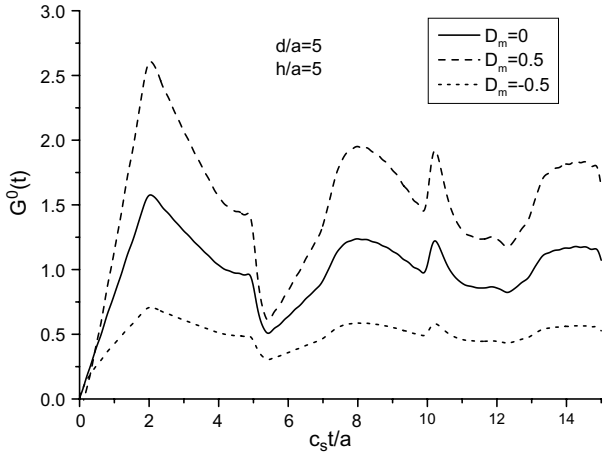


Fig. 8. Variation of $G^0(t)$ against $c_s t/a$ with $d/a = 5$, $h/a = 5$, $D_m = 0.5$, 0, −0.5 under the impermeable assumption.

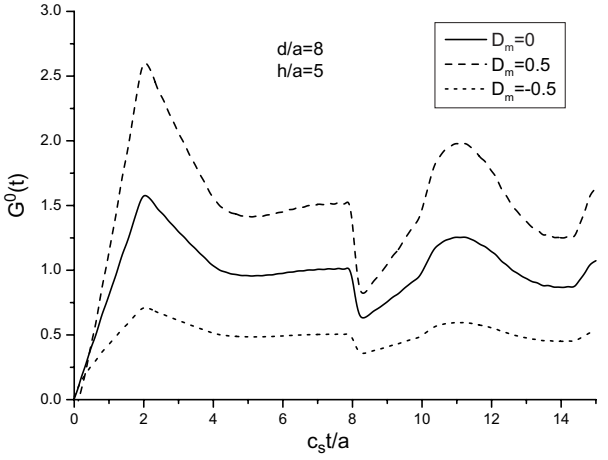


Fig. 9. Variation of $G^0(t)$ against $c_s t/a$ with $d/a = 8$, $h/a = 5$, $D_m = 0.5$, 0, −0.5 under the impermeable assumption.

impacts, which indicates that positive electric impacts promote crack growth, and negative electric impacts hinder crack growth, in accordance with the static analysis and experimental phenomena (Park and Sun, 1995). Additionally, it should be noted that the response curves of $G^0(t)$ for $D_m = -0.5$ are flatter than those for $D_m = 0, 0.5$. In effect, it can be concluded from (68) that $G^0(t) = 0$ for $D_m = -1$, which reveals that the strain vanishes, and of course the cracks do not propagate in this case. (Fig. 10)

Under a positive electric displacement, the effect of the layer thickness on the normalized SERR $G^0(t)$ for two impermeable surface cracks spaced by a fixed distance is illustrated in Fig. 10. By inspection, it is found from Fig. 10 that for two surface cracks spaced by a fixed distance, the transient response is independent of the thickness of the piezoelectric layer during the early stage of the action of impact, and relies on the thickness after a period of time.

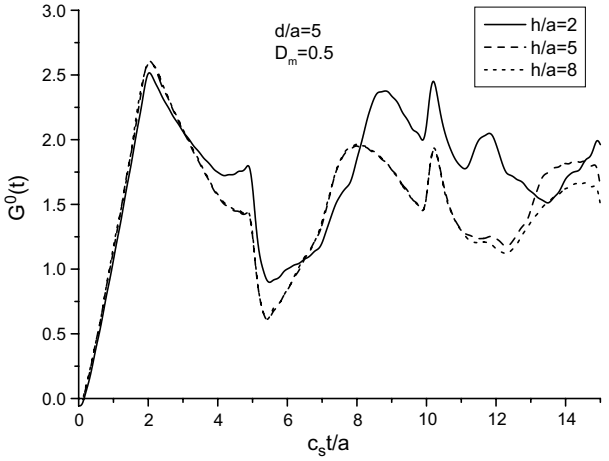


Fig. 10. Response of $G^0(t)$ under $D_m = 0.5$ for different thicknesses under the impermeable assumption.

## 6. Conclusions

The transient problem involving two surface cracks in a piezoelectric ceramic layer is analyzed under the action of antiplane mechanical and inplane electric impacts. Using integral transform techniques, the mixed boundary value problem is converted into singular integral equations. Dynamic field intensity factors in the Laplace transform domain are obtained. By solving numerically the resulting singular integral equations and performing numerically the inverse Laplace transform, the dynamic stress intensity factor and strain energy release rate are presented graphically to show the effects of the geometric parameters and the material properties. The dynamic interaction of two cracks, and cracks with free boundaries are analyzed and explained in detail.

## Acknowledgements

This work was supported by the National Natural Science Foundation of China under Grant No. 10272043, the Natural Science Foundation of Hunan Province under Grant No. 02JJY4004, and the Korea Institute of Science and Technology Evaluation and Planning.

## References

Chen, Z.-T., Karihaloo, B.L., 1999. Dynamic response of a cracked piezoelectric ceramic under arbitrary electro-mechanical impact. International Journal of Solids and Structures 36, 5125–5133.

Chen, Z.-T., Meguid, S.A., 2000. The transient response of a piezoelectric strip with a vertical crack under electromechanical impact load. International Journal of Solids and Structures 37, 6051–6062.

Crump, K.S., 1976. Numerical inversion of Laplace transforms using a Fourier series approximation. Journal of the Association for Computing Machinery 23, 89–96.

Dascalu, C., Maugin, G.A., 1995. On the dynamic fracture of piezoelectric materials. Quarterly Journal of Mechanics and Applied Mathematics 48, 237–255.

Dieulesaint, E., Royer, G.A., 1980. Elastic Waves in Solids. John Wiley & Sons, New York.

Erdogan, F., Gupta, G.D., Cook, T.S., 1973. Numerical solution of singular integral equations. In: Sih, G.C. (Ed.), Mechanics of Fracture, vol. 1, pp. 368–425.

Gu, B., Wang, X., Yu, S., Gross, D., 2002. Transient response of a Griffith crack between dissimilar piezoelectric layers under anti-plane mechanical and in-plane electrical impacts. Engineering Fracture Mechanics 69, 565–576.
Khutoryansky, N.M., Sosa, H., 1995. Dynamic representation formula and fundamental solutions for piezoelectricity. International Journal of Solids and Structures 32, 3307–3325.
Kwon, S.M., Lee, K.Y., 2001. Edge cracked piezoelectric ceramic block under electromechanical impact loading. International Journal of Fracture 112, 139–150.
Li, S., Mataga, P.A., 1996a. Dynamic crack propagation in piezoelectric materials—part I. Electrode solution. Journal of Mechanics and Physics Solids 44, 1799–1830.
Li, S., Mataga, P.A., 1996b. Dynamic crack propagation in piezoelectric materials—part II. Vacuum solution. Journal of Mechanics and Physics Solids 44, 1831–1866.
Li, X.-F., 2001. Transient response of a piezoelectric material with a semi-infinite mode-III crack under impact loads. International Journal of Fracture 111, 119–130.
Li, X.-F., Fan, T.-Y., 2002. Transient analysis of a piezoelectric strip with a permeable crack under anti-plane impact loads. International Journal of Engineering Science 40, 131–143.
Li, X.-F., Tang, G.J., 2003. Transient response of a piezoelectric ceramic strip with an eccentric crack under electromechanical impacts. International Journal of Solids and Structures 40, 3571–3588.
Meguid, S.A., Chen, Z.T., 2001. Transient response of a finite piezoelectric strip containing coplanar insulating cracks under electromechanical impact. Mechanics of Materials 33, 85–96.
Meguid, S.A., Zhao, X., 2002. The interface crack problem of bonded piezoelectric and elastic half-space under transient electromechanical loads. Journal of Applied Mechanics 69, 244–253.
Mueller, V., Zhang, Q.M., 1998. Shear response of lead zirconate titanate piezoceramics. Journal of Applied Physics 83, 3754–3761.
Narris, A.N., 1994. Dynamic Green's functions in anisotropic piezoelectric, thermoelastic and poroelastic solids. Proceeding of Royal Society of London. Ser. A. 447, 175–186.
Pak, Y.E., 1990. Crack extension force in a piezoelectric material. Journal of Applied Mechanics 57, 647–653.
Park, S., Sun, C.T., 1995. Fracture criteria for piezoelectric ceramics. Journal of the American Ceramic Society 78, 1475–1480.
Rao, S.S., Sunar, M., 1994. Piezoelectricity and its use in disturbance sensing and control of flexible structures: a survey. Applied Mechanics Review 47, 113–123.
Shindo, Y., Narita, F., Ozawa, E., 1999. Impact response of a finite crack in an orthotropic piezoelectric ceramic. Acta Mechanica 137, 99–107.
Shin, J.W., Kwon, S.M., Lee, K.Y., 2001. An eccentric crack in a piezoelectric strip under anti-plane shear impact loading. International Journal of Solids and Structures 38, 1483–1494.
Sosa, H., Khutoryansky, N., 2001. Further analysis of the transient dynamic response of piezoelectric bodies subjected to electric impulses. International Journal of Solids and Structures 38, 2101–2114.
Suo, Z., Kuo, C.-M., Barnett, D.M., Willis, J.R., 1992. Fracture mechanics for piezoelectric ceramics. Journal of Mechanics and Physics Solids 40, 739–765.
Theocaris, P.S., Ioakimids, N.I., 1977. Numerical integration methods for the solution of singular integral equations. Quarterly of Applied Mathematics 35, 173–183.
Tsou, H.S., Bergman, L.A., 1998. Dynamics and Control of Distributed Systems. Cambridge University Press, Cambridge.
Uchino, K., 1998. Materials issues in design and performance of piezoelectric actuators: an overview. Acta Materialia 46, 3745–3753.
Wang, B.L., Han, J.C., Du, S.Y., 1998. Dynamic response for non-homogeneous piezoelectric medium with multiple cracks. Engineering Fracture Mechanics 61, 607–617.
Wang, B.L., Noda, N., 2001. Transient loaded smart laminate with two piezoelectric layers bonded to an elastic layer. Engineering Fracture Mechanics 68, 1003–1012.
Wang, X., Yu, S., 2000. Transient response of a crack in piezoelectric strip subjected to the mechanical and electrical impacts: mode-III problem. International Journal of Solids and Structures 37, 5795–5808.
Yang, W., 2001. Mechatronic Reliability. Tsinghua University Press, Beijing (in Chinese).